EDGEWOOD CHEMICAL BIOLOGICAL CENTER
U.S. ARMY RESEARCH, DEVELOPMENT AND ENGINEERING COMMAND
Aberdeen Proving Ground, MD 21010-5424

ECBC-TR-993

INFRARED EXTINCTION COEFFICIENTS OF AEROSOLIZED CONDUCTIVE FLAKE POWDERS AND FLAKE SUSPENSIONS HAVING A ZERO-TRUNCATED POISSON SIZE DISTRIBUTION

Brendan G. DeLacy
Janon F. Embury

RESEARCH AND TECHNOLOGY DIRECTORATE

November 2012

Disclaimer

The findings in this report are not to be construed as an official Department of the Army position unless so designated by other authorizing documents.

REPORT DOCUMENTATION PAGE

Form Approved
OMB No. 0704-0188

1. REPORT DATE *(DD-MM-YYYY)*	2. REPORT TYPE	3. DATES COVERED *(From – To)*
XX-11-2012	Final	Jan 2009 - Dec-2011

4. TITLE AND SUBTITLE
Infrared Extinction Coefficients of Aerosolized Conductive Flake Powders and Flake Suspensions having a Zero-Truncated Poisson Size Distribution

5a. CONTRACT NUMBER

5b. GRANT NUMBER

5c. PROGRAM ELEMENT NUMBER
62622A552

6. AUTHOR(S)
DeLacy, Brendan G.; and Embury, Janon F.

5d. PROJECT NUMBER

5e. TASK NUMBER

5f. WORK UNIT NUMBER

7. PERFORMING ORGANIZATION NAME(S) AND ADDRESS(ES)
Director, ECBC, ATTN: RDCB-DRT-S, APG, MD 21010-5424

8. PERFORMING ORGANIZATION REPORT NUMBER
ECBC-TR-993

9. SPONSORING/MONITORING AGENCY NAME(S) AND ADDRESS(ES)

10. SPONSORING/MONITOR'S ACRONYM(S)

11. SPONSOR/MONITOR'S REPORT NUMBER(S)

12. DISTRIBUTION / AVAILABILITY STATEMENT
Approved for public release; distribution is unlimited.

13. SUPPLEMENTARY NOTES

14. ABSTRACT (Maximum 200 words)

High-aspect-ratio aluminum, graphite, and brass flake powders were disseminated into an aerosol chamber and their infrared extinction coefficients were measured. Suspensions, which were prepared by stirring and sonicating the flake powders into ethanol, were also disseminated into the aerosol chamber as droplets that quickly evaporated, leaving aerosols that were used for extinction measurement. A twin-fluid atomizing nozzle was used to disseminate all materials into a stirred 190 m^3 cylindrical aerosol chamber. After dispersion by the nozzle and thorough chamber mixing with a low speed fan, spectral aerosol transmittance and concentration were simultaneously measured to obtain spectral extinction coefficients. Zero-truncated Poisson distributions were used to describe the population of flakes in aerosol particles that were produced by evaporation of suspension droplets. The geometric optics expression for flake extinction coefficient also provided a way to obtain the average agglomerate thickness from aerosol extinction coefficient measurements. This information was then interpreted in terms of single flakes and flake aggregates that coalesced when suspension droplets evaporated and briefly coagulated. Aerosols formed by disseminating dry powders formed agglomerates consisting of 1.3 to 3 flakes per particle, and dried suspension droplet aerosols formed larger agglomerates consisting of 2 to 5 flakes per particle.

15. SUBJECT TERMS

Extinction	Obscuration	Poisson distribution
Dissemination	Aerosols	Zero-truncated distribution

16. SECURITY CLASSIFICATION OF:			17. LIMITATION OF ABSTRACT	18. NUMBER OF PAGES	19a. NAME OF RESPONSIBLE PERSON
a. REPORT	b. ABSTRACT	c. THIS PAGE			Renu B. Rastogi
U	U	U	UU	34	19b. TELEPHONE NUMBER *(include area code)* (410) 436-7545

Blank

PREFACE

The work described in this report was authorized under program element no. 62622A552. This work was started in January 2009 and completed in December 2011.

The use of either trade or manufacturers' names in this report does not constitute an official endorsement of any commercial products. This report may not be cited for purposes of advertisement.

This report has been approved for public release.

Acknowledgments

The authors would like to acknowledge Christine Franklin (Science Applications International Corporation) for administrative support in preparing this document.

Blank

CONTENTS

FIGURES

TABLES

INFRARED EXTINCTION COEFFICIENTS OF AEROSOLIZED CONDUCTIVE FLAKE POWDERS AND FLAKE SUSPENSIONS HAVING A ZERO-TRUNCATED POISSON SIZE DISTRIBUTION

1. INTRODUCTION

Suspensions of high-aspect-ratio aluminum, graphite, and brass flake powders, with thicknesses in the nanometer range, were disseminated into an aerosol chamber and their infrared extinction coefficients (extinction cross-section per mass) were measured. Suspensions with varying concentrations were prepared by stirring and sonicating the powders in ethanol. A twin-fluid atomizing nozzle, consisting of a jet of the suspensions surrounded by an annular sonic air jet, was used to disseminate all materials into a stirred, 190 m^3, dished-end, vertical, cylindrical aerosol chamber. The suspensions were disseminated as droplets that quickly evaporated leaving solid particulate aerosols. After thoroughly mixing the aerosols in the chamber using a low speed fan, the spectral transmittance and concentration of the aerosols were simultaneously measured to obtain spectral extinction coefficients. Serving as controls in the study, dry forms of the powders were also disseminated using a twin-fluid nozzle, and the infrared extinctions were subsequently measured.

Determining the impact of droplet flake population on the infrared extinction coefficient was fundamental to this study. It was hypothesized that droplets with excess flakes would negatively impact the infrared extinction coefficient, if the flakes agglomerate during droplet evaporation. Therefore, various suspension concentrations were evaluated during the study to vary the average flake population contained in each droplet.

Zero-truncated Poisson distributions were used to describe the population of flakes in aerosol particles that were produced by evaporation of the suspension. This distribution was then combined with the geometric optics expression for flake extinction coefficients. By combining these two expressions, the average overall thicknesses of the agglomerated aerosol particle ensembles were determined from the aerosol extinction coefficient measurements. The data were then interpreted in terms of single flakes and flake aggregates that coalesced when suspension droplets evaporated, briefly coagulated, and then exited as a region of highly concentrated aerosol particles near the source.

2. BACKGROUND

Aerosol infrared extinction is one of the variables controlling radiative transfer and imaging through the atmosphere. At visible wavelengths, the eye perceives an image as a result of color contrasts that consist of differences in luminance and chromaticity (hue and saturation). These differences are perceptible below the Nyquist spatial frequency that is set by the packing density of retinal photoreceptors in the eye.[1–5] Thermal imagers are used to convert infrared spectral radiance scene contrasts into color contrasts on the visual display. The differences can be normalized in a variety of ways to yield various expressions for contrast or color difference.

An image observed through an aerosol cloud consists of the transmitted original image, attenuated by scatter and absorption, plus ambient light that is scattered or emitted along the line of sight within the cloud (path radiance) and superimposed onto the transmitted image. Contrast transmittance through the cloud is frequently used to quantify these two effects upon visibility through a cloud. It is defined as the ratio of image contrast as seen through a cloud divided by image contrast without the cloud present. Contrast transmittance is a function of the extinction coefficient, single-scatter albedo, asymmetry parameter, concentration pathlength product, emission, and ambient illumination.[6] The extinction coefficient is generally more important than single-scatter albedo and asymmetry parameter in controlling contrast transmittance. The metal flakes used in this study were exceptional because they possessed a particularly high infrared extinction coefficient that made image obscuration possible with a minimum quantity of flake material. One engineering goal of this study was to aerosolize and deagglomerate these flake materials to maximize extinction coefficients and dissemination yields (fraction of material that becomes airborne).

3. EXTINCTION COEFFICIENT

The extinction coefficient is defined in terms of the beam attenuation of electromagnetic radiation due to scattering and absorption as the beam traverses a medium. Beam attenuation depends on the complex refractive index, size, shape, orientation, and concentration of the particles, as well as the wavelength and polarization of incident radiation. The aerosol mass extinction coefficient α (m^2/g) is related to the beam transmittance T through an aerosol cloud by

$$T = e^{-\int \alpha c dl} \tag{1}$$

where c is the concentration of particles (g/m^3) along the line of sight, and dl is the path length increment.[7] In a stirred aerosol chamber, the aerosol extinction coefficient and concentration can be made uniform along any line-of-sight length L (m), and the extinction coefficient becomes

$$\alpha = \frac{\ln\left(1/T\right)}{cL} \tag{2}$$

This equation provides a convenient and compatible set of units with beam transmittance in the range $0 \le T \le 1$. The aerosol mass extinction coefficient is related to the aerosol volume extinction coefficient α_V (m^2/cc) by the density ρ (g/cc), of the aerosolized material, as described in eq 3.

$$\alpha_V = \alpha \times \rho \tag{3}$$

Mass extinction coefficient (referred to as the *extinction coefficient*) depends on extinction efficiency factor Q, geometric cross-section G, and particle volume V as given in the relationship[7]

$$\alpha = \frac{QG}{\rho V} \tag{4}$$

Averaging over aerosol particle orientation Ω, shape, and size (volume) distributions, the extinction coefficient is written as

$$\left\langle \left\langle \left\langle \alpha \right\rangle_{\Omega} \right\rangle_{\text{shape}} \right\rangle_{V} = \frac{\left\langle \left\langle \left\langle QG \right\rangle_{\Omega} \right\rangle_{\text{shape}} \right\rangle_{V}}{\rho \left\langle \left\langle V \right\rangle_{\text{shape}} \right\rangle_{V}} = \frac{Cov(QG) + \left\langle \left\langle \left\langle Q \right\rangle_{\Omega} \right\rangle_{\text{shape}} \right\rangle_{V} \times \left\langle \left\langle \left\langle G \right\rangle_{\Omega} \right\rangle_{\text{shape}} \right\rangle_{V}}{\rho \left\langle \left\langle V \right\rangle_{\text{shape}} \right\rangle_{V}} \tag{5}$$

where *Cov(QG)* is the covariance averaged over orientation, shape, and size distributions. Generally, numerical solutions for Q are obtained using Mie calculations for homogeneous spherical particles.

In the case of homogeneous nonspherical particles, calculations are based on the extended boundary condition or *T*-matrix method, developed by Waterman and popularized by Barber, Yeh, and Mishchenko.[8–13] Electromagnetic cross-sections for inhomogeneous or composite particles of any shape are often computed using the discrete dipole approximation developed and popularized by Draine and Flatau.[14,15] However, physical insight into extinction coefficient is gained most quickly by using simple analytical approximate solutions for Q, where dependence upon particle properties can be seen upon inspection. Even when dependence is not obvious, simple solutions lead to rapid calculating and plotting of the extinction coefficient as a function of particle properties. For example, simple solutions can also be used to rapidly determine optimum properties that can maximize the extinction coefficient. In the geometric optics-scattering regime, $Q = 2$, and, therefore, $Cov(QG) = 0$. Convex particles have a geometric cross-section averaged over a random orientation equal to one-fourth their surface area, $G = S/4$. Therefore, the average extinction coefficient for a convex particle in the geometric optics regime can be written as

$$\left\langle \left\langle \left\langle \alpha \right\rangle_{\Omega} \right\rangle_{\text{shape}} \right\rangle_{V} \xrightarrow{\text{GeometricOptics\&Convex}} \frac{\left\langle \left\langle S \right\rangle_{\text{shape}} \right\rangle_{V}}{2\rho \left\langle \left\langle V \right\rangle_{\text{shape}} \right\rangle_{V}} \tag{6}$$

In the case of a high-aspect-ratio flake having thickness t (μm), the edge area can be ignored so that surface area S is equal to twice the flake face area F. Hence, $S = 2F$ and the volume is $V = tF$. Substituting these values into eq 6 for the extinction coefficient, results in the extinction coefficient for a flake in the geometric optics limit as described in eq 7.

$$\langle \alpha \rangle = \frac{1}{\rho\, t} \tag{7}$$

Extinction coefficient spectra for measured conductive flakes are flat throughout the visible though infrared regions to wavelengths close to twice the flake major dimensions. At wavelengths beyond twice the major dimensions of the flake face area, the extinction coefficient drops with increasing wavelength and Raleigh scattering begins.[16] Thus, the geometric optics result can be extended across the resonance region as long as the flakes are opaque and the extinction cross-section is averaged over a large ensemble of randomly oriented and somewhat shape- and size-distributed flakes. This is the case for the three conductive flake powders tested in this study where the major dimensions for the flakes were 10–17.5 μm, and the transmissometer line-of-sight in the aerosol chamber was several meters long. Because flakes tend to form compact stacks when they agglomerate, it is also possible to use the geometric optics result to relate the total agglomerate thickness to the flake agglomerate extinction coefficient.

Measuring aerosol cloud extinction is more practical and less complicated than predicting cloud extinction based on the extinction measurements of individual particles. This is because considerable time would be needed to accumulate data sufficient to predict the average extinction coefficient of a typical aerosol cloud containing an ensemble of particles with multiple sizes, shapes, and orientation distributions.

4. DISSEMINATION METHOD

Dissemination techniques used to produce an aerosol cloud play a vital role in controlling the aerosol dispersion and degree of agglomeration. The performance of a dissemination method is generally characterized using two measurements: yield and particle size distribution. As long as particle sizes do not significantly impact the lifetimes of interest for the aerosol cloud, measurement of the particle size can be avoided, and measurement of the extinction coefficient can suffice. *Yield* is a measurement of dissemination efficiency and is defined as the ratio of the mass aerosolized to the mass of material that entered the dissemination device (see eq 8). Yield indicates the presence of large aggregates that do not remain in the air long enough to be collected on a filter sample that is used to measure concentration.

$$Yield = \frac{mass\,of\ airborne\,material}{initial\ mass\,of\ material} \tag{8}$$

The dissemination of a solid material may be achieved in dry powder form or in wet suspension form. For this study, a twin-fluid atomizing nozzle, consisting of a jet of these powders or suspensions that were surrounded by an annular sonic air jet, was used to disseminate all materials into a dished end, cylindrical aerosol chamber with a 190 m^3 volume.[17,18] The dry powders were aerosolized using a pneumatic redispersion technique in which the powder was loosely fed into an airstream and subsequently dispersed through the nozzle. The wet suspensions were disseminated by siphoning the liquid through a feed line toward the nozzle that formed it into a liquid jet or sheet. The liquid jet or sheet was then atomized through the

interaction with a high velocity gas. The velocity and pressure of the air at the nozzle head, the solvent properties, and the siphoning rate all played a role in the diameter of the aerosol droplets that were produced. The nozzle produced droplets that acted as a carrier for the flakes. Upon evaporation of the droplet, the flakes were airborne for a period of time within the chamber where the attenuation properties could be subsequently measured.

An ideal scenario for the dissemination of a wet suspension is one in which each flake is transported from the nozzle into the chamber in one droplet. The droplet will evaporate after a period of time, and the remaining flake will be mixed in the chamber as a solid aerosol particulate. In a non-ideal situation, two or more flakes could be carried in one droplet. Due to capillary and van der Waals forces, the propensity of the flakes to agglomerate as the droplet evaporates increases. Aggregation has a direct effect on particle size, yield, and extinction. Agglomerated particles tend to exhibit decreased extinction coefficients in the infrared region. This reduction is proportional to the surface area-to-volume ratio of the agglomerate, except in the low-frequency region where agglomerate size is small when compared with wavelength. Therefore, the particle population in a droplet is a significant factor to consider when disseminating a suspension with an atomizing nozzle. In statistical terms, the number of particles in a drop follows a Poisson distribution, which represents the Gaussian distribution in the limit of large mean values.

5. FLAKE POPULATION DISTRIBUTIONS IN EVAPORATING SUSPENSION DROPLETS AND DROPLET LIFETIME

The population distribution of flakes or hard stack flake aggregates in suspension droplets is given by the Poisson distribution, where *P(k)* is the probability of k flakes or stack aggregates residing in a droplet, with mean $\langle k \rangle$ equal to variance $[(k - \langle k \rangle)^2]$:

$$P(k) = \frac{\lambda^k e^{-\lambda}}{k!}; \ \sum_0^\infty P(k) = 1 \tag{9}$$

$$\langle k \rangle = \lambda \tag{10}$$

$$[(k - \langle k \rangle)^2] = \lambda \tag{11}$$

Upon droplet evaporation, we assume that the *k* flakes or stack aggregates in a droplet coalesce to form a single aerosol particle consisting of *k* flakes or stack aggregates. Then the population distribution of flakes or stack aggregates in aerosol particles can be written as a zero-truncated Poisson distribution, where P_{ZTP} *(k)* is the probability of *k* flakes or stack aggregates residing in an aerosol particle with mean $\langle k \rangle_{\mathrm{ZTP}}$ and variance $[(k - \langle k \rangle)]^2{}_{ZTP}$ expressed in eq 12 in terms of the Poisson distribution mean λ in eqs 9–11[19]

$$P_{\mathrm{ZTP}}(k) = \frac{\lambda^k}{(e^\lambda - 1)k!}; \quad \sum_1^\infty P_{\mathrm{ZTP}}(k) = 1 \tag{12}$$

$$\langle k \rangle_{\mathrm{ZTP}} = \frac{\lambda}{1 - e^{-\lambda}} \tag{13}$$

$$[(k-\langle k\rangle)^2]_{\mathrm{ZTP}} = \frac{\lambda[1-(\lambda+1)e^{-\lambda}]}{(1-e^{-\lambda})^2} \tag{14}$$

To determine the total number of droplets, one must first determine the average volume of the droplets. This is achieved by measuring the diameter of the droplets using a particle-sizing instrument. The diameter of the droplet can subsequently be used to calculate the volume of the droplet using the volume of a sphere equation. By knowing the initial volume of solvent used in the suspension and by calculating the average droplet volume, the number of droplets may be deduced. The number of flakes may be estimated by first calculating the volume of the flake from known dimensions. The volume of a flake is modeled on the volume of a cylinder, where the major dimension of the flake is assumed to be the cylindrical diameter, and the thickness of the flake is assumed to be the cylindrical height. The flake volume can subsequently be converted to the flake mass using the material density. The estimated number of flakes can then be determined by dividing the initial mass of powder by the estimated mass of a flake.

An additional factor to consider during the dissemination of a suspension using an atomizing nozzle is the evaporation rate of the droplet. The lifetime of a droplet should be sufficiently short so that deposition of the droplet does not occur prior to evaporation. In 1877, James Maxwell derived the original equation for the evaporation of a droplet as a function of time as

$$I = 2\pi D d(c_s - c_l) \tag{15}$$

where I is the evaporation rate as a function of droplet diameter d, D is the diffusion coefficient of the solvent vapor, c_l is the concentration of vapor a large distance away from the droplet, and c_s is the saturation concentration.[12] To account for temperature changes in a droplet due to condensation or evaporation, eq 15 is altered to reflect a steady-state condition (constant evaporation rate and temperature) described by

$$T_l - T_s = \frac{DML}{RK_t}\left(\frac{p_s}{T_s} - \frac{p_l}{T_l}\right) \tag{16}$$

where T_l and p_l are the temperature and partial pressure of vapor away from the drop, respectively, and T_s and p_s are the temperature and vapor pressure at the surface of the droplet, respectively.[12] M is the molecular weight (gmol) and R has a value of 62,360 cm^3·mmHg/(K·mol). L is the latent heat of evaporation (cal/g) and K_t is the thermal conductivity of the vapor (cal/cm/s/K).

In the previous equations, the reduction in droplet diameter as a droplet evaporates was not accounted for. Langmuir's equation uses a quasi-stationary condition to provide a crude estimate of the lifetime of a drop in

$$\tau_0 = \frac{\rho RT\left(d^2 - {d_0}^2\right)}{8DM\left(p_s - p_l\right)} = \rho RT\left(d^2 - {d_0}^2\right)\left\{\left\{8DMp_\infty\left(T_l\right)\left[\frac{p_s}{p_\infty\left(T_l\right)} - S\right]\right\}\right. \quad (17)$$

where τ_0 is the time for a droplet of diameter d to evaporate to diameter d_0 when the partial pressure in the surrounding medium is p_l.[12] S is the saturation ratio and $p_s = p_\infty(T_l)$ is used in place of computing a value from eq 17.

6. INSTRUMENTAL METHODS AND MATERIALS

A study was undertaken to evaluate the effects of suspension concentration on extinction and yield measurements. Aluminum, brass, and graphite flakes were evaluated in the study. The aluminum flakes (Reynolds Metals Company, Louisville, KY), brass flakes (U.S. Bronze Powders, Inc., Flemington, NJ), and graphite flakes (Asbury Carbons, Asbury, NJ) had average major dimensions of 10, 10, and 17.5 μm, respectively and average thicknesses of 100, 80, and 100 nm, respectively. Prior to initiating the wet suspension study, the extinction coefficients of the dry powder forms of aluminum, brass, and graphite were first determined. Dispersion of the dry powder form was achieved using a pneumatic redispersion technique in which the powder was loosely fed into an airstream and subsequently dispersed through a nozzle.

In the suspension concentration study, aluminum, brass, and graphite flakes were suspended in ethanol and disseminated into a 190 m^3 chamber using an air-atomizing nozzle. Aluminum suspension concentrations (0.01, 0.02, 0.033, 0.04, and 0.048 g/mL), brass suspension concentrations (0.002, 0.01, 0.02, 0.10, and 0.20 g/mL), and graphite suspension concentrations (0.002, 0.005, 0.015, 0.041, and 0.06 g/mL) were evaluated. The nozzle used in the experiments (model 1/4J, Spraying Systems Co., Wheaton, IL) required a liquid line and an air source for the production of droplets. The liquid suspension was supplied via a siphon, and 110 psi of air was supplied to the nozzle. The suspensions were housed in 1 L vacuum filtration flasks. A variable vacuum line was connected to the flask so that a negative pressure within the flask could be applied. The amount of negative pressure within the flask had a direct influence on the droplet size produced by the nozzle.

The suspension concentrations (mass of powder per volume of liquid) were varied so that a range of particle populations was produced during the study. The particle populations were estimated by calculating the number of droplets and flakes using the rationale described in Section 5. The estimated particle population did not imply that there are a specific number of flakes in each individual droplet. It merely provided a statistical average of the particle population in each droplet. A laser diffraction-based particle-sizing instrument (Helos Model, Sympatec GmbH, Clausthal-Zellerfeld, Germany) was used to measure the diameters of atomized droplets before significant evaporation and to measure the major dimensions of aerosol particles in dispersed powders.

Based on eqs 15–17, the calculated droplet lifetimes for 1 and 10 μm ethanol droplets were 0.0003 and 0.03 s, respectively.[17] The size of the droplets varied from 5 to 10 μm

in this study. Therefore, the lifetimes of the droplets were sufficiently short to ensure droplet evaporation and subsequent aerosolization of flakes prior to deposition.

All powders and suspensions were disseminated into a cylindrical chamber with a volume of 190 m^3 (6 m diameter, 6.8 m height). A diagram of the chamber is provided in Figure 1.

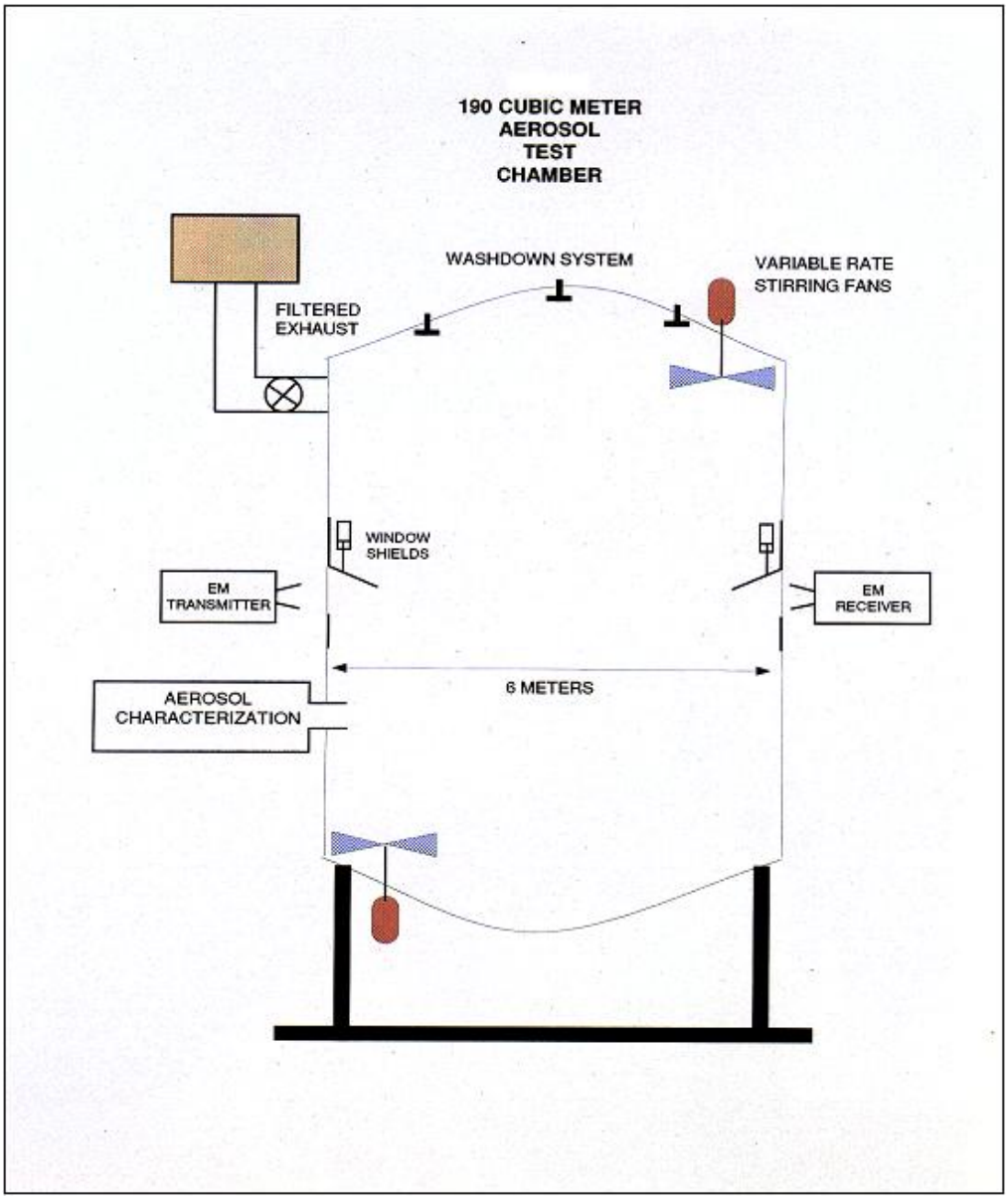

Figure 1. Aerosol test chamber.

The chamber was equipped with a stirring fan to provide a homogeneous mixture of flakes throughout. Transmission in the infrared region (2.5 to 20 μm) was determined using a Jasco Fourier transform infrared spectroscopy (FTIR) spectrometer (model FT/IR-6100, Jasco Inc., Easton, MD). A path length of 6 m was used in all calculations because the FTIR source

was placed 6 m away from the detector. The FTIR source and detector were both placed at a height of 3.4 m. The concentration of flake material within the chamber was determined by taking an aliquot of air from the chamber. This was achieved by pulling air samples from the chamber onto a glass filter for a 120 s time period. The mass accumulated on the filter was weighed and the volume of air was measured using a flow meter (model FMA-1618A, Omega Engineering, Inc., Stamford, CT). Transmission and concentration were not measured until homogeneity in the chamber was achieved after dissemination. Homogeneity was assumed when a steady state in laser transmission was observed. A 672 nm laser diode (Newport, Mountain View, CA) was used in the laser transmissometry system.

An additional study was undertaken to determine the effects of droplet size on extinction and yield while holding suspension concentration constant. This study involved the dissemination of aluminum flakes (Al flake 40XD, Reynolds Aluminum Co.) in ethanol using the same experimental setup previously described in this section. However, to vary the droplet size, the pressure within the vacuum filtration flask was varied using a ball valve. A decrease in flask pressure resulted in a decrease in the droplet size produced.

7. RESULTS AND DISCUSSION

Figures 2, 3, and 4 provide the extinction spectra for aluminum, brass, and graphite flakes when dispersed in both dry powder and wet suspension forms. These materials were evaluated in bulk powder form to provide a baseline comparison to the wet suspension forms of the same materials. Absorption due to ethanol was observed in the spectra for all wet suspension samples. This absorption was particularly pronounced in the 6 to 11 μm region. To circumvent this effect, the absorption due to ethanol was corrected for in all extinction spectra. Additionally, the plotted data were filtered using a running average.

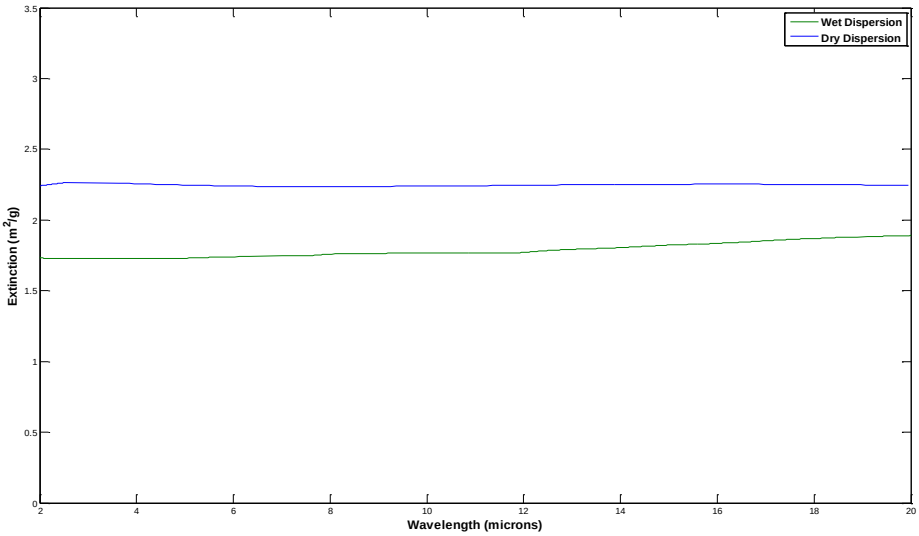

Figure 2. Extinction spectra for aluminum flakes when dispersed as a dry powder and as a wet suspension.

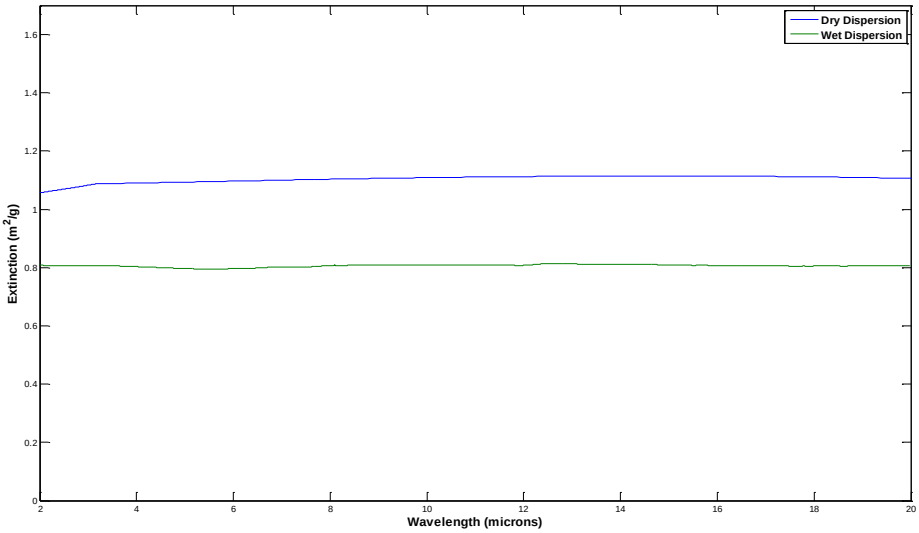

Figure 3. Extinction spectra for brass flakes when dispersed as a dry powder and as a wet suspension.

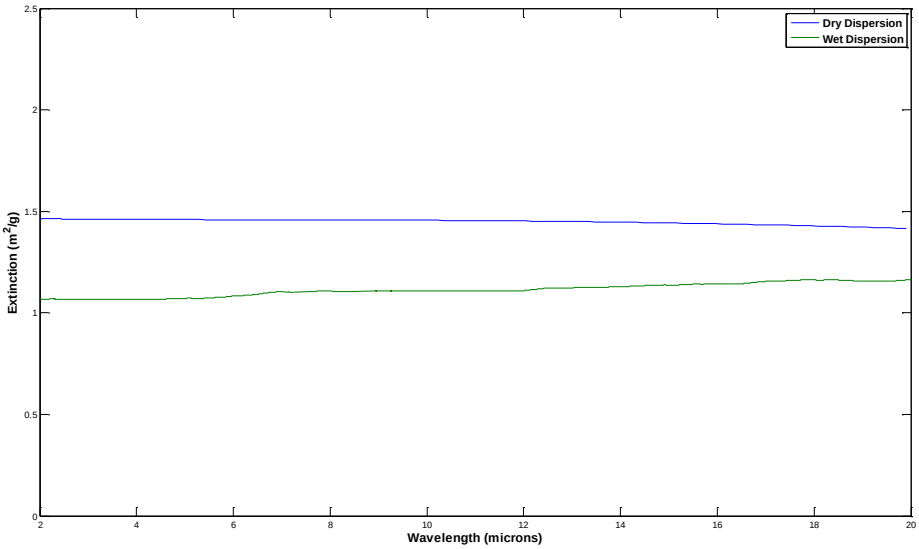

Figure 4. Extinction spectra for graphite flakes when dispersed as a dry powder and as a wet suspension.

Tables 1, 2, and 3 provide a summary of extinction and yield results obtained for the evaluation of aluminum flake, brass flake, and graphite flake wet suspensions. An average droplet size of 7.5 μm was used for all results displayed in Tables 1–3. The extinction and yield factor were determined for all experiments. Due to considerable absorption of the solvent at certain wavelength regions in the corrected spectra, average extinction values for the spectra were calculated in the 4–6 and 12–20 μm regions.

The air and flask pressures used for the nozzle parameters were held constant for these measurements to ensure that the droplet size was held constant.

Table 1. Extinction and Yield Results for Aluminum Flake Suspension

Concentration (g/mL)	Number of Flakes per Droplet	Yield Factor	Average Extinction (m^2/g)	95% Confidence Interval
0.01	0.25	0.75	1.60	0.010
0.02	0.49	0.75	1.40	0.014
0.033	0.82	0.72	1.30	0.021
0.04	0.99	0.68	1.27	0.007
0.048	1.19	0.57	1.12	0.007

Table 2. Extinction and Yield Results for Brass Flake Suspension

Concentration (g/mL)	Number of Flakes per Droplet	Yield Factor	Average Extinction (m^2/g)	95% Confidence Interval
0.002	0.02	0.92	0.79	0.020
0.01	0.10	0.87	0.73	0.006
0.02	0.20	0.78	0.57	0.006
0.10	0.98	0.58	0.60	0.004
0.20	1.96	0.50	0.50	0.003

Table 3. Extinction and Yield Results for Graphite Flake Suspension

Concentration (g/mL)	Number of Flakes per Droplet	Yield Factor	Average Extinction (m^2/g)	95% Confidence Interval
0.002	0.02	0.799	1.32	0.022
0.005	0.05	0.711	1.22	0.012
0.015	0.16	0.702	0.99	0.007
0.041	0.43	0.658	0.80	0.003
0.06	0.62	0.652	0.83	0.002

Inspection of Tables 1, 2, and 3 reveals that there was a general decline in both the yield factor and extinction for each material as the particle population per droplet increased. These trends could be related to the fact that as the particle population increased, the likelihood of two or more flakes residing in a droplet also increased. Similarly, as the likelihood of multiple particles in a droplet increased, so did the tendency to agglomerate. When two or more flakes reside in one droplet, capillary and van der Waals forces play major roles in agglomeration during droplet evaporation. The decrease in extinction could be attributed to the fact that agglomerated particles decrease the surface area-to-volume ratio, which is one of the important parameters that influence the attenuation of infrared radiation. The decrease in yield could be attributed to increased settling velocities of the largest aggregates, produced by a combination of flake coalescence during droplet evaporation and coagulation among evaporating droplets. Increased settling velocity due to coalescence alone would increase the stirred settling-concentration decay rate, but would not increase it enough to account for the tabulated yield

differences corresponding to concentration decreases during the short time between dissemination and aerosol mass concentration filter sampling.

Table 4 provides a summary of extinction and yield results for the experiments that dealt with the effect of the variability in droplet size. For this study, the concentrations of aluminum flake suspensions were held at a constant 0.04 g/mL. The droplet size was varied by varying the negative pressure within the flask. Median droplet sizes of 10.0, 8.0, 7.0, 5.5, and 5.0 μm were obtained when applying flask pressures of 0, –1.0, –2.0, –3.0, and –4.0 in.Hg, respectively. Again, as in Tables 1–3, the yield and extinction coefficient generally decrease as the number of flakes per droplet increases. Flake aggregates produced by coalescence during droplet evaporation can be expected to have lower extinction coefficients than individual flakes due to the decrease in the surface area-to-volume ratio. Additionally, settling velocities of the largest aggregates, produced by a combination of coalescence and coagulation, can be expected to settle out quickly enough to reduce measured yield.

Table 4. The Impact of Droplet Size on Extinction and Yield Results for Aluminum Flakes

Concentration (g/mL)	Average Droplet Size	Number of Flakes per Droplet	Yield Factor	Average Extinction (m^2/g)	95% Confidence Interval
0.04	10.0	0.99	0.680	1.27	0.007
0.04	8.0	0.51	0.737	1.34	0.001
0.04	7.0	0.34	0.833	1.63	0.006
0.04	5.5	0.16	0.820	1.52	0.015
0.04	5.0	0.12	0.813	1.27	0.033

Table 5 summarizes the values for flake thicknesses t_{SEM}, determined by scanning electron microscopy (SEM) image analysis, and dry powder aerosol aggregate thicknesses t_{PA}, determined by inversion of the extinction coefficient $\alpha_{\text{Dry Powder}}$ measurements of disseminated dry powders using geometric optics. All three powders contained flake stack aggregates which, as indicated by the extinction coefficient, were not all broken up into individual flakes by the combination of air turbulence-driven shear forces and interparticle collisions encountered while passing through the dissemination nozzle.

Table 5. Flake Properties and Dry Powder Stack Aggregate Thicknesses

Flake Powder Material	Flake Major Dimensions (μm)	Particle Density, ρ (g/cc)	SEM Flake Thickness, t_{SEM} (μm)	Disseminated Dry Powder Aerosol ExtinctionCoefficient, $\alpha_{\text{Dry Powder}}$ (m^2/g)	Disseminated Dry Powder Aerosol Aggregate Thickness $t_{PA} = \frac{1}{\rho \alpha_{\text{Dry Powder}}}$
Aluminum	10	2.7	0.100	2.25	0.165
Brass	10	8.5	0.080	1.10	0.107
Graphite	17.5	2.2	0.100	1.45	0.313

Tables 6, 7, and 8 summarize the theoretical analysis of all suspension droplet aerosol measurements appearing in Tables 1–5.

Analysis of aluminum, brass, and graphite flakes using SEM images showed no flake crumpling or folding; therefore, measurements were interpreted in terms of stack aggregates of flakes that were also evident in these images. The strength of the bond among the flakes is unknown but might be broken by a combination of ultrasonic dispersion to form suspensions followed by pneumatic aerosolization. When a suspension droplet evaporates, the flakes, or the hard flake stack aggregates in the droplet, coalesce to form an aerosol particle. Table 6 provides the theoretical number of flakes per droplet because of a combination of coalescence of the particles within a droplet as it dries, plus coagulation among drying droplets. All calculated values were based on the flake thicknesses determined using SEM analysis and the measured extinction values that are provided in column 4 of Table 6. The number of flakes per aerosol particle due to coalescence, $\langle k \rangle_{\mathrm{ZTP}}^{\mathrm{SEM}}$, and the factor increases in this number due to coagulation, $\gamma_{\mathrm{Coag}}^{\mathrm{SEM}}$, are provided in columns 3 and 5, respectively.

Table 6. Coalescence and Coagulation of Flakes in Evaporating Droplets Based on Flake Thickness Observed with SEM

Material	λ_{SEM} Number of Flakes per Drop	$\langle k \rangle_{\mathrm{ZTP}}^{\mathrm{SEM}}$ Coalesced Number of Flakes per Aerosol Particle after Droplet Evaporation	α Aerosol Extinction Coefficient (m^2/g)	$\gamma_{\mathrm{Coag}}^{\mathrm{SEM}}$ Factor Increase in Flakes per Aerosol Particle Due to Coagulation
Aluminum	0.12	1.06	1.27	2.75
Aluminum	0.16	1.08	1.52	2.26
Aluminum	0.25	1.13	1.60	2.05
Aluminum	0.34	1.18	1.63	1.92
Aluminum	0.49	1.26	1.40	2.10
Aluminum	0.51	1.28	1.34	2.16
Aluminum	0.82	1.47	1.30	1.94
Aluminum	0.99	1.58	1.27	1.85
Aluminum	1.19	1.71	1.12	1.94
Brass	0.02	1.01	0.79	1.84
Brass	0.10	1.05	0.73	1.91
Brass	0.20	1.1	0.57	2.35
Brass	0.98	1.57	0.60	1.56
Brass	1.96	2.28	0.50	1.29
Graphite	0.02	1.01	1.32	3.41
Graphite	0.05	1.03	1.22	3.64
Graphite	0.16	1.08	0.99	4.25
Graphite	0.43	1.23	0.80	4.62
Graphite	0.62	1.34	0.83	4.09

Table 7 is similar to Table 6, with the exception that powder aggregate thickness from Table 5 was used, instead of SEM flake thickness (hard powder aggregates are assumed to survive sonication, producing the dispersion), to calculate the number of aggregates per aerosol particle due to coalescence, $\langle k \rangle_{\mathrm{ZTP}}^{\mathrm{PA}}$, and the factor increase of that value due to coagulation, $\gamma_{\mathrm{Coag}}^{\mathrm{PA}}$. The information in Table 8 was compiled on the assumption that there was no prior knowledge of flake or hard-stack aggregate thickness and there was no coagulation among drying droplets. Only the coalescence of flakes or stack aggregates that survived sonication should have produced the dispersion.

The numbers of flakes or aggregates per droplet ($\langle k \rangle_{\mathrm{ZTP}}^{\mathrm{SEM}}$ or $\langle k \rangle_{\mathrm{ZTP}}^{\mathrm{PA}}$), in coalesced aerosol particles, followed the zero-truncated Poisson distribution. This distribution corresponds to the droplet Poisson mean number of flakes or hard aggregates per droplet (λ_{SEM} or λ_{PA}). Taking into consideration the coalescence of single flakes or stack aggregates would not explain the observed extinction coefficients provided in Tables 6 and 7. It was, therefore, necessary to include coagulation in the calculations. We believe the droplets contained essentially powder aggregates, rather than individual flakes, because there was less variability in the factor increase due to coagulation, $\gamma_{\mathrm{Coag}}^{\mathrm{PA}}$, of powder aggregates than there was in the factor increase of flakes per droplet, $\gamma_{\mathrm{Coag}}^{\mathrm{SEM}}$. This variability should be independent of the material tested because dissemination conditions were replicated for all tests. Calculations to obtain the values in Tables 6, 7, and 8 are summarized below.

$$\lambda_{\mathrm{PA}} = \left(\frac{t_{\mathrm{SEM}}}{t_{\mathrm{PA}}}\right)\lambda_{\mathrm{SEM}};\ \lambda_{\mathrm{SA}} = \left(\frac{t_{\mathrm{SEM}}}{t_{\mathrm{SA}}}\right)\lambda_{\mathrm{SEM}} \tag{18}$$

$$t_{\mathrm{Coal\,\&\,Coag}}^{\mathrm{Flake}} = \langle k \rangle_{\mathrm{ZTP}}^{\mathrm{SEM}} \cdot \gamma_{\mathrm{Coag}}^{\mathrm{SEM}} . t_{\mathrm{SEM}} = \frac{1}{\rho\alpha} \xrightarrow{\text{solving}} \gamma_{\mathrm{Coag}}^{\mathrm{SEM}} = \frac{1}{\langle k \rangle_{\mathrm{ZTP}}^{\mathrm{SEM}} \rho\alpha t_{\mathrm{SEM}}} \tag{19}$$

$$t_{\mathrm{Coal\,\&\,Coag}}^{\mathrm{PA}} = \langle k \rangle_{\mathrm{ZTP}}^{\mathrm{PA}} \cdot \gamma_{\mathrm{Coag}}^{\mathrm{PA}} . t_{\mathrm{PA}} = \frac{1}{\rho\alpha} \xrightarrow{\text{solving}} \gamma_{\mathrm{Coag}}^{\mathrm{PA}} = \frac{1}{\langle k \rangle_{\mathrm{ZTP}}^{\mathrm{PA}} \rho\alpha t_{\mathrm{PA}}} \tag{20}$$

$$t_{\mathrm{Coal}}^{\mathrm{SA}} = \langle k \rangle_{\mathrm{ZTP}}^{\mathrm{SA}} t_{\mathrm{SA}} = \frac{1}{\rho\alpha} \xrightarrow{\text{Solving}} t_{\mathrm{SA}} = \frac{1}{\langle k \rangle_{\mathrm{ZTP}}^{\mathrm{SA}} \rho\alpha} \xrightarrow{\text{Solving}} t_{\mathrm{SA}} = \frac{\lambda_{\mathrm{SEM}} t_{\mathrm{SEM}}}{\ln\left(\frac{1}{1-\lambda_{\mathrm{SEM}} t_{\mathrm{SEM}} \rho\alpha}\right)} \tag{21}$$

Table 7. Coalescence and Coagulation of Aggregates in Evaporating Droplets Based on Calculated Powder Aggregate Thickness (t_{PA}) from Table 5

Material	λ_{PA} Powder Aggregates per Drop	$\langle k \rangle_{ZTP}^{PA}$ Coalesced Number of Powder Aggregates per Aerosol Particle after Droplet Evaporation	α Aerosol Extinction Coefficient (m^2/g)	γ_{Coag}^{PA} Factor Increase in Powder Aggregates per Aerosol Particle Due to Coagulation
Aluminum	0.07	1.04	1.27	1.70
Aluminum	0.10	1.05	1.52	1.41
Aluminum	0.15	1.08	1.60	1.30
Aluminum	0.21	1.11	1.63	1.24
Aluminum	0.30	1.16	1.40	1.38
Aluminum	0.31	1.16	1.34	1.44
Aluminum	0.50	1.27	1.30	1.36
Aluminum	0.60	1.33	1.27	1.33
Aluminum	0.72	1.40	1.12	1.43
Brass	0.02	1.01	0.79	1.38
Brass	0.08	1.04	0.73	1.49
Brass	0.15	1.08	0.57	1.79
Brass	0.73	1.41	0.60	1.30
Brass	1.47	1.91	0.50	1.15
Graphite	0.01	1.00	1.32	1.10
Graphite	0.02	1.01	1.22	1.18
Graphite	0.05	1.03	0.99	1.42
Graphite	0.14	1.07	0.80	1.70
Graphite	0.20	1.10	0.83	1.59

Table 8. Coalescence Ignoring Coagulation of Aggregates in Evaporating Droplets

Material	t_{SA} Sonication Aggregate Thickness (μm)
Aluminum	0.07
Aluminum	0.10
Aluminum	0.15
Aluminum	0.21
Aluminum	0.30
Aluminum	0.31
Aluminum	0.50
Aluminum	0.60
Aluminum	0.72
Brass	0.02
Brass	0.08
Brass	0.15
Brass	0.73
Brass	1.47
Graphite	0.01
Graphite	0.02
Graphite	0.05
Graphite	0.14
Graphite	0.20

8. DRY FLAKE AEROSOL PARTICLE-SETTLING STUDIES

Our aerosol particle-settling studies consisted of sequential transmissometer spectral scans, along with sequential filter concentration measurements, taken over periods of time that allowed significant aerosol concentration decay. The goals of these studies are to track extinction coefficient changes expected as larger aerodynamic diameter flakes fall out and to determine aerosol particle-settling velocities, which provide an independent measure of flake major dimensions as explained in the Stokes flow and geometric optics regimes.

Measurements of chamber aerosol concentration and spectral transmission were used to calculate aerosol spectral extinction coefficient and, ultimately, flake thicknesses. Additional measurements of aerosol concentration as a function of time can be used to calculate aerosol particle-settling velocities based on the chamber stirred-settling equation.[20] That velocity can then be related to flake dimensions through an expression for Stokes drag on an oblate spheroid in the disk or high aspect-ratio limit.[21] The flake major dimension was subsequently determined by substituting into that drag expression a value for flake thickness that was based on simultaneous extinction coefficient measurements. Conductive flake aerosol extinction

coefficients in the geometric optics regime increase as flake thickness decreases. This is generally observed in conductive flake-settling studies and can be explained when there is a positive correlation between flake thickness and major dimension. This can lead to thicker flakes having larger settling velocities and, therefore, larger aerodynamic diameters. Thus, aerosol concentration and spectral transmission must be measured simultaneously as a function of time to perform an inversion of both major and minor (thickness) flake dimensions.

The stirred settling expression for aerosol concentration c, as a function of initial concentration c_0, time τ, chamber height H, and aerosol particle-settling velocity υ, is

$$c = c_0 \exp\left[-\frac{\upsilon \tau}{H}\right] \tag{22}$$

or

$$\upsilon = \frac{H}{\tau} \ln\left[\frac{c_0}{c}\right] \tag{23}$$

Aerosols are almost always polydispersed so that settling velocities should be computed incrementally

$$\upsilon_i = \frac{H}{\tau_{i+1} - \tau_i} \ln\left[\frac{c_i}{c_{i+1}}\right] \tag{24}$$

from a sequence of concentration measurements $c_0 > c_1 > c_2 > \ldots > c_N$ where $c_i \equiv c(\tau_i)$ and $\tau_0 > \tau_1 > \tau_2 > \ldots > \tau_N$ will decrease over time.

Here, aerosol concentration was maintained uniformly throughout the chamber by gentle stirring. The stirring removed a negligible quantity of aerosol by impaction on the fan blades and turbulence-induced impaction on chamber walls. This settling velocity, based on aerosol concentration decay measurements, can be compared to an expression for settling velocity as a function of flake dimensions based on Stokes drag to determine flake dimensions.

The settling velocity was estimated by balancing the aerodynamic drag force against the gravitational force that acts on an aerosol particle. A spherical aerosol particle of diameter d, moving through air at a velocity υ, encounters a drag force in the Stokes regime (Reynolds number, $\mathrm{Re} << 1$) equal to $3\pi d\mu\upsilon$, where μ is the dynamic viscosity of air. The drag force F_D, acting on a disk of equal volume, can be written in terms of a proportionality factor f_E [21] as

$$F_D = f_E 3\pi d\mu\upsilon \tag{25}$$

The proportionality factor f_E is a function of disk orientation relative to the velocity and a function of disk aspect ratio $E = \frac{d_\parallel}{d_\perp}$, where $d_\parallel$ is the disk dimension along the symmetry axis (thickness) and $d_\perp$ is the disk equatorial (major)-axis dimension.[23] The equivalent volume sphere diameter d can be written in terms of $d_\parallel$, $d_\perp$, and E

$$d = d_\parallel E^{-\frac{2}{3}} = d_\perp E^{\frac{1}{3}} \tag{26}$$

For velocity parallel to the symmetry axis

$$f_{E\parallel} = \frac{8}{3\pi} E^{-\frac{1}{3}} \tag{27}$$

and for velocity perpendicular to the symmetry axis

$$f_{E\perp} = \frac{16}{9\pi} E^{-\frac{1}{3}} \tag{28}$$

Averaging over random orientations

$$\frac{3}{\langle f_E \rangle} = \frac{1}{f_{E||}} + \frac{2}{f_{E\perp}} \tag{29}$$

In the case of a randomly oriented disk, the average becomes

$$\frac{3}{\langle f_E \rangle} = \frac{3\pi}{8} E^{\frac{1}{3}} + \frac{18\pi}{16} E^{\frac{1}{3}} = \frac{3\pi}{2} E^{\frac{1}{3}} \tag{30}$$

and

$$\langle f_E \rangle = \frac{2}{\pi} E^{-\frac{1}{3}} \tag{31}$$

$$F_D = 6 d_\perp \mu \upsilon \tag{32}$$

when the weight of the disk (mg)

$$mg = \rho d_\parallel \pi \frac{d_\perp{}^2}{4} g \tag{33}$$

is balanced against this drag force we can solve for the disk-settling velocity

$$\upsilon = \frac{\pi \rho d_{\parallel} d_{\perp} g}{24\mu} \tag{34}$$

Substituting settling velocities υ_i, based on sequential concentration measurements c_i into this expression, we can solve for disk major dimension $d_{\perp}$ representative of the population of flakes remaining airborne

$$d_{\perp} = \frac{24\mu H}{\pi \rho d_{\parallel} g\left(\tau_{i+1} - \tau_i\right)} \ln\left[\frac{c_i}{c_{i+1}}\right] \tag{35}$$

in terms of the thickness $d_{\parallel}$, corresponding to the extinction coefficient representative of that population.

The validity of this expression can be checked by calculating the corresponding Reynolds number

$$\mathrm{Re} \equiv \frac{\rho_f \upsilon d}{\mu} = \frac{\upsilon d}{\nu} \tag{36}$$

where ρ_f is the density and $\nu \equiv \frac{\mu}{\rho_f}$ is the kinematic viscosity of air (0.14 cm^2/s). Using Table 9 to find the combination of velocity and major dimension that produces the largest Reynolds number, we find that $\mathrm{Re} = \frac{(0.15)(0.0113)}{0.14} = 0.0121$, which is well within the Stokes flow regime. If the corresponding equivalent volume sphere diameter were used instead of flake major dimension, the Reynolds number would be even smaller. Thus, all Reynolds numbers are in the Stokes flow regime, and the expression relating settling velocity to disk dimensions is applicable.

Table 9. Settling to Determine Flake Dry Powder Thickness Distribution and Major Dimensions

Material	Time After Dissemination (s)	Aerosol Concentration (g/m^3)	Settling Velocity (cm/s)	$\alpha_{\text{DryPowder}}$ Extinction Coefficient (m^2/g)	$t_{PA} = \frac{1}{\rho \alpha_{\text{DryPowder}}}$ Powder Aggregate Thickness (μm)	Flake Major Dimension (μm)
Aluminum	0	0.03789	NA	2.25	0.165	NA
Aluminum	2,799	0.01749	0.188	*	*	*
Aluminum	9,290	0.00519	0.127	4.4	0.084	78
Aluminum	10,760	0.00375	0.150	5.4	0.069	113
Aluminum	16,645	0.00175	0.088	6.4	0.058	79
Brass	0	0.05211	NA	1.10	0.107	NA
Brass	1,785	0.03534	0.148	*	*	*
Brass	5,955	0.01660	0.123	*	*	*
Brass	8,037	0.01231	0.098	1.38	0.085	19
Brass	9,454	0.00944	0.127	1.63	0.072	29
Graphite	0	0.04642	NA	1.45	0.313	NA
Graphite	6,160	0.02137	0.086	2.8	0.162	34
Graphite	10,950	0.01285	0.072	3.2	0.142	32
Graphite	15,549	0.00722	0.085	4.7	0.097	56

It is evident from the data presented in Table 9 that the fraction 0.00175/0.03789 (about 5%) of the disseminated aluminum powder that remained in the air after 16,645 s had an extinction coefficient of 6.4 m^2/g, which was nearly three times greater than the disseminated value of 2.25 m^2/g. Similarly, the fraction of disseminated brass powder that remained in the air after 9454 s was 0.00944/0.05211 (about 18%), and it had an extinction coefficient of 1.63 m^2/g, which was nearly 1.5 times greater than the disseminated value of 1.1 m^2/g. Likewise, the fraction 0.00722/ 0.04642 (about 16%) of the disseminated graphite powder that remained in the air after 15,549 s had an extinction coefficient of 4.7 m^2/g, which was more than three times greater than the disseminated value of 1.45 m^2/g. It should also be noted that all major flake dimensions obtained in Table 9 exceeded those stated by the manufacturer in Table 5.

9. CONCLUSIONS

The zero-truncated Poisson distribution represents the number distribution of primary particles in an aggregated aerosol, formed by primary-particle coalescence during evaporation of aerosolized suspension droplets that contain a Poisson distribution of primary particles. Geometric optic inversions of the extinction coefficient were used to obtain ensemble average flake stack aggregate thicknesses. Aerosol data was then analyzed using this distribution function and inversion from the viewpoint that the suspensions contained single flakes and flake aggregates, which were typical of those encountered after dry powder dissemination. These suspension droplets evidently coagulated during the evaporation process to reach a final agglomerated aerosol particle thickness. This thickness was a roughly 1.4-fold increase in

agglomerate size beyond that formed by hard flake aggregate coalescence caused by droplet evaporation. Primary particles, consisting of hard flake stack aggregates typical of those in the dry powder, appeared to have survived the ultrasonic dispersion process to result in an increase in the coagulation factor value that was more consistent than that obtained if flake primary particles were present. Data were also analyzed from the viewpoint that there was no coagulation, only coalescence. The primary flake stack aggregate thicknesses that were calculated in this analysis were considered to be unrealistically large considering that all suspensions were sonicated. Reductions in the extinction coefficient caused by flakes folding onto themselves and crumpling were not considered because neither event was evident in the SEM analysis, which revealed only flake stacking. Dry powder aerosol particle-settling studies demonstrated a threefold increase in the extinction coefficient for aluminum and graphite powders and a 50% increase for brass powder using 5–18% of the thinnest flakes.

Blank

LITERATURE CITED

1. Sharma, G.; Wu, W.; Dalal, E. The CIEDE2000 Color-Difference Formula: Implementation Notes, Supplementary Test Data, and Mathematical Observations. *Color Res. Appl.* **2005**, *30*(1), 21–30.

2. Duntley, S.Q.; Gordon, J.I.; Taylor, J.H.; White, C.T.; Boileau, A.R.; Tyler, J.E.; Austin, R.W.; Harris, J.L. Visibility. *Appl. Optics* **1964**, *3*(5), 549–598.

3. Vimal, R.L.P. Spatial Color Contrast Matching: Broad-Bandpass Functions and the Flattening Effect. *Vision Res.* **2000**, *40*, 3231–3243.

4. Wikipedia, Contrast (vision). http://en.wikipedia.org/wiki/Contrast_(vision) (accessed March 2012).

5. NASA Ames Research Center, Luminance Contrast. http://colorusage.arc.nasa.gov/luminance_cont.php (accessed March 2012).

6. Embury, J. *Emissive Versus Attenuating Smokes;* ECBC-TR-225; U.S. Army Edgewood Chemical Biological Center: Aberdeen Proving Ground, MD, 2002; UNCLASSIFIED Report (AD-A400816).

7. Bohren, C.F.; Huffman, D.R. *Absorption and Scattering of Light by Small Particles*; Wiley-VCH: Weinheim, Germany, 2004.

8. Waterman, P.C. Matrix Formulation of FO Electromagnetic Scattering. *Proc. IEEE* **1965**, *53*, 805–812.

9. Waterman P.C. Matrix Methods in Potential Theory and Electromagnetic Scattering. *J. Appl. Phys.* **1979**, *50*, 4550–4565.

10. Waterman P.C. New Formulation of Acoustic Scattering *Alta. Freq*. **1969**, *38*, 348–352.

11. Waterman P.C. Symmetry, Unitarity, and Geometry in Electromagnetic Scattering. *Phys. Rev. D*. **1971**, *3*, 825–839.

12. Barber, P.W.; Yeh, C. Scattering of Electromagnetic Waves by Arbitrarily Shaped Dielectric Bodies. *Appl. Opt.* **1975**, *14*, 2864–2872.

13. Mishchenko, M.I.; Travis L.D. T-Matrix Computations of Light-Scattering by Large Spheroidal Particles. *Opt. Comm.* **1994**, *109* (1–2), 16–21.

14. Draine, B.T. The Discrete-Dipole Approximation and Its Application to Interstellar Graphite Grains. *Astrophys. J.* **1988**, *333* (2), 848–872.

15. Draine, B.T.; Flatau, P.J. **2004**, *User Guide for the Discrete Dipole Approximation Code DDSCAT.6.1*, *Freeware.* http://arxiv.org/abs/astro-ph/0409262 (accessed March 2012).

16. Embury, J.F. Extinction by Clouds Consisting of Polydisperse and Randomly Oriented Non-Spherical Particles at Arbitrary Wavelengths. *Opt. Eng.* **1983**, *22* (1), 71–77.

17. Hinds, W.C., *Aerosol Technology: Properties, Behavior, and Measurement of Airborne Particles*; John Wiley & Sons, Inc.: Hoboken, NJ, 1999.

18. Fritsching, U. Spray Systems. In *Multiphase Flow Handbook;* Crowe, C.T., Ed.; Chapter 8; CRC-Press: Boca Raton, FL, 2006; pp. 8.1–8.100.

19. Klugman, S.; Panjer, H.H.; Willmost, G.E. *Loss Models: From Data to Decisions;* 3rd ed.; John Wiley & Sons, Inc.: Hoboken, NJ, 2008.

20. Fuchs, N.A. *The Mechanics of Aerosols*; Pergamon Press: Oxford, U.K., 1964.

21. Loth, E. Drag of Non-Spherical Solid Particles of Regular and Irregular Shape. *Powder Technol.* **2008**, *182* (3), 342–353.


EDGEWOOD CHEMICAL BIOLOGICAL CENTER
A U.S. Army RDECOM Laboratory